ELSEVIER

Contents lists available at ScienceDirect

Separation and Purification Technology

journal homepage: www.elsevier.com/locate/seppur



Separating carbon dioxide from natural gas by a hollow fiber membrane contactor with various absorbents: Numerical investigation of membrane wettability

Hamed Rahnema^a, Amin Etminan^{b,*}, Sara Barati^{c,*}, Kevin Pope^b

ARTICLE INFO

Keywords: Absorbent kinetics Carbon dioxide absorption COMSOL Multiphysics Wetting percentage

ABSTRACT

This study investigated CO_2 separation from natural gas using hollow fiber membrane contactors, focusing on the combined effects of membrane wettability and absorbent type on separation efficiency. Unlike prior studies that primarily examined dry or fully wetted membranes, we explored intermediate wetting conditions (20 %–60%) to simulate realistic operational scenarios over time. Three absorbents—monoethanolamine (MEA), piperazine (PZ), and triethanolamine (TEA)—with distinct reaction kinetics were evaluated. The results indicated that under dry conditions, all absorbents achieve near-100 % CO_2 removal due to fast reaction kinetics relative to gas flow. However, under wetted conditions (20 %–60 %), absorbent type significantly influenced performance, with PZ (the fastest-reacting) removing up to 15 % of CO_2 at the maximum gas velocity (3.3 m/s), compared to just 5 % for TEA (the slowest-reacting) at 60 % wetting, while at 20 % wetting, the removal efficiencies were 51 % for PZ and 38 % for TEA. Furthermore, we modeled long-term performance decline due to membrane aging and wetting, providing novel insights for industrial applications. This work advances sustainable gas separation technologies by elucidating the interplay of wettability, absorbent kinetics, and temporal dynamics, and by addressing key gaps in previous research.

1. Introduction

Natural gas consists predominantly of methane (CH_4), up to 70–90 %, but also comprises other constituents, such as carbon dioxide (CO_2) [1]. Natural gas appliances, such as furnaces and stoves, emit CO_2 through combustion and CH_4 directly into the atmosphere due to leaks and incomplete combustion [2–4]. In many cases, it is beneficial to remove the CO_2 prior to natural gas utilization [5,6]. Different methods, such as adsorption, absorption, and membrane separation technologies, are extensively employed for gas purification [7–9]. Among these, membrane separation systems have garnered significant attention due to their high performance in various separation applications [10].

Hollow fiber membranes stand out for their exceptional performance, making them preferable to other membrane configurations. Hollow fiber membrane systems have recently become a focus of research for the separation of carbon dioxide from many gas streams

[11,12]. A hollow fiber membrane separation system consists of three parts: shell, membrane, and tube side. The membrane acts as a barrier, preventing mixing between the two fluids and selectively allowing specific components to pass through the membrane. To separate $\rm CO_2$ using a hollow fiber membrane contactor, allows only carbon dioxide molecules to pass through its pores. Research efforts to improve the efficiency of membrane contactor systems in separation processes have focused on optimizing process conditions, membrane properties, and structural designs. However, the membrane or separator often determines the lifespan of the system. As a result, research has predominantly concentrated on improving membrane properties and structures [13–17].

Polymeric membranes such as polyether sulfone, polyamide, and polyvinyl fluoride are used to separate carbon dioxide from various gas mixtures. Water repellency, resistance to heat and pressure, and simplifying the membrane structure to reduce production costs are crucial in selecting appropriate membrane materials for separation

E-mail addresses: aetminan@mun.ca (A. Etminan), sara.barati1367@yahoo.com (S. Barati).

a Department of Chemical Engineering, University of Toledo, Toledo, OH, USA

b Department of Mechanical and Mechatronics Engineering, Faculty of Engineering and Applied Science, Memorial University of Newfoundland (MUN), St. John's, NL A1B 3X5, Canada

c University of São Paulo, São Carlos Institute of Chemistry, Av. Trabalhador São-Carlense, 400, 13560-970 São Carlos, SP, Brazil

^{*} Corresponding authors.

Nomenclature Greek Symbols porosity ε English Letters void volume inside the module ω concentration ($mol \cdot m^{-3}$) C_i θ contact angle (degree) concentration in the outer-tube (mol•m⁻³) liquid's surface tension (N/m) $C_{i-shell}$ concentration in the inner-tube ($mol \cdot m^{-3}$) C_{i-tube} Subscripts/Superscripts $C_{i-membrane}$ concentration in the membrane (mol•m⁻³) inlet boundary inlet gas flow rate in shell (m³•s⁻¹) Q_{in} g gas diffusion coefficient (m²•s⁻¹) D_i liquid 1 CO₂ mass transfer flux (mol•m⁻²•s⁻¹) J_i membrane m length of the module (m) L outlet boundary out gas solubility (mol•mol⁻¹) m_i pore of the membrane p number of fiber n w gas flow rate at the inlet (m³•s⁻¹) Q_{in} gas flow rate at the outlet $(m^3 \cdot s^{-1})$ Q_{out} Abberviations radial coordinate (m) r **HFMC** hollow fiber membrane contactor membrane pore radius (m) r_p MEA monoethanolamine radius of dried part of membrane (m) R_{dry} normalized root mean square error nRMSE reaction rate (mol•s⁻¹) R_i PARDISO parallel direct sparse solver R_{wet} radius of wet part of membrane (m) polyvinylidene fluoride **PVDF** Ttemperature (K) PZpiperazine average velocity in the outer tube $(m \cdot s^{-1})$ и TEA triethanolamine velocity (m•s⁻¹)

processes. Among the investigated membranes for carbon dioxide separation, polyvinylidene fluoride (PVDF) membranes have gained attention due to their relatively low production cost and favorable properties [6,13,18–21]. Besides membrane type, the choice of absorbent also significantly affects process efficiency, which are generally classified as either physical or chemical absorbents [22,23].

Chemical absorbents offer notable benefits, including higher absorption capacity and rate of reaction compared to physical absorbents, which provide chemical absorbents an important benefit when the absorption efficiency is the most important factor [24–26]. Given the high purity of methane and the challenge of achieving efficient separation, experimental and modeling studies on removing carbon dioxide from methane are of great importance. Hence, extensive research has been conducted in modeling and experimental phases to introduce and examine suitable membranes, absorbents, and operating conditions for this process [6,25,27].

Nakhjiri and Heydarinasab [28] numerically investigated CO₂ separation from a CO₂/CH₄ mixture in a hollow fiber membrane contactor (HFMC) using absorbents such as ethylenediamine (EDA), 2-(1-piperazinyl)-ethylamine (PZEA), and potassium sarcosinate (PS). The results demonstrated that the absorbent type plays a critical role in the separation process, with PZEA achieving the highest CO2 removal efficiency (88.75 %), followed by PS (82.2 %) and EDA (81 %). Abdolahi-Mansoorkhani and Seddighi [19] developed a mathematical model to study the simultaneous removal of CO2 and H2S from natural gas using a PVDF membrane enhanced with calcium carbonate (CaCO₃) nanoparticles. The results showed that adding nanoparticles to the membrane modifies membrane porosity and surface characteristics, significantly impacting removal efficiency. In another study, they investigated the effect of membrane wettability at 50 % wetting on removal efficiency, finding that wettability increases mass transfer resistance and drastically reduces separation performance (from 75 % under non-wetted conditions to just 8 % under partially wetted conditions) [18]. Most modeling studies have focused on the effect of absorbent type on CO2 separation efficiency in membrane systems, whereas only a few have investigated the long-term effects of membrane wettability. The combined analysis of wettability and absorbent type remains largely unexplored. Gilassi and Rahmanian [29] developed a two-dimensional model for CO₂ separation from a CO2/N2 gas mixture using a hollow fiber membrane contactor

(HFMC). Their study focused on the effects of various amine solutions, such as monoethanolamine (MEA), diethanolamine (DEA), and nmethyldiethanolamine (MDEA) as chemical absorbents for $\rm CO_2$ separation. Results showed that MEA provided the highest separation efficiency.

Additionally, some modeling efforts have been conducted for both fully dry and fully wetted membrane conditions to evaluate the effect of membrane wettability on performance [29–32]. However, only a limited number of studies have examined different degrees of membrane wetting, and these were typically conducted using a physical absorbent, a single chemical absorbent, or several absorbents from the same group with similar reaction rates. The effect of absorbent type during different stages of membrane wetting has not been investigated.

This paper investigates the impact of membrane wetting, which depends on the membrane's physical and chemical properties, on the performance of hollow fiber membrane contactors used for CO_2 separation from natural gas, using numerical analysis in COMSOL Multiphysics. The effects of absorbent type and membrane wetting are investigated for MEA, piperazine (PZ), and triethanolamine (TEA). In partially or fully wetted membranes, the absorbent fills the voids, enabling chemical reactions between the absorbent and CO_2 within the membrane structure. In contrast, in non-wetted membranes, chemical reactions occur only at the interface between the membrane and the absorbent phase.

2. Formulation of numerical predictions

Fig. 1 illustrates a hollow fiber membrane contactor system designed to separate carbon dioxide from sour natural gas. The system has a shell and a bundle of hollow fibers with walls made of PVDF, which act as the membrane (separator). The fibers are arranged in parallel and uniform boundary conditions are applied at the inlet, outlet, and lateral surfaces. Therefore, a single fiber is simulated under the assumption that its behavior is representative of the entire module. In this system, the gas mixture passes through the shell, and the absorbent (liquid) circulates through the tube in a counter-current configuration.

The system's geometric parameters and the membranes' physical specifications are presented in Table 1.

Based on Happel's free surface model [33], Fig. 2(b), we consider a

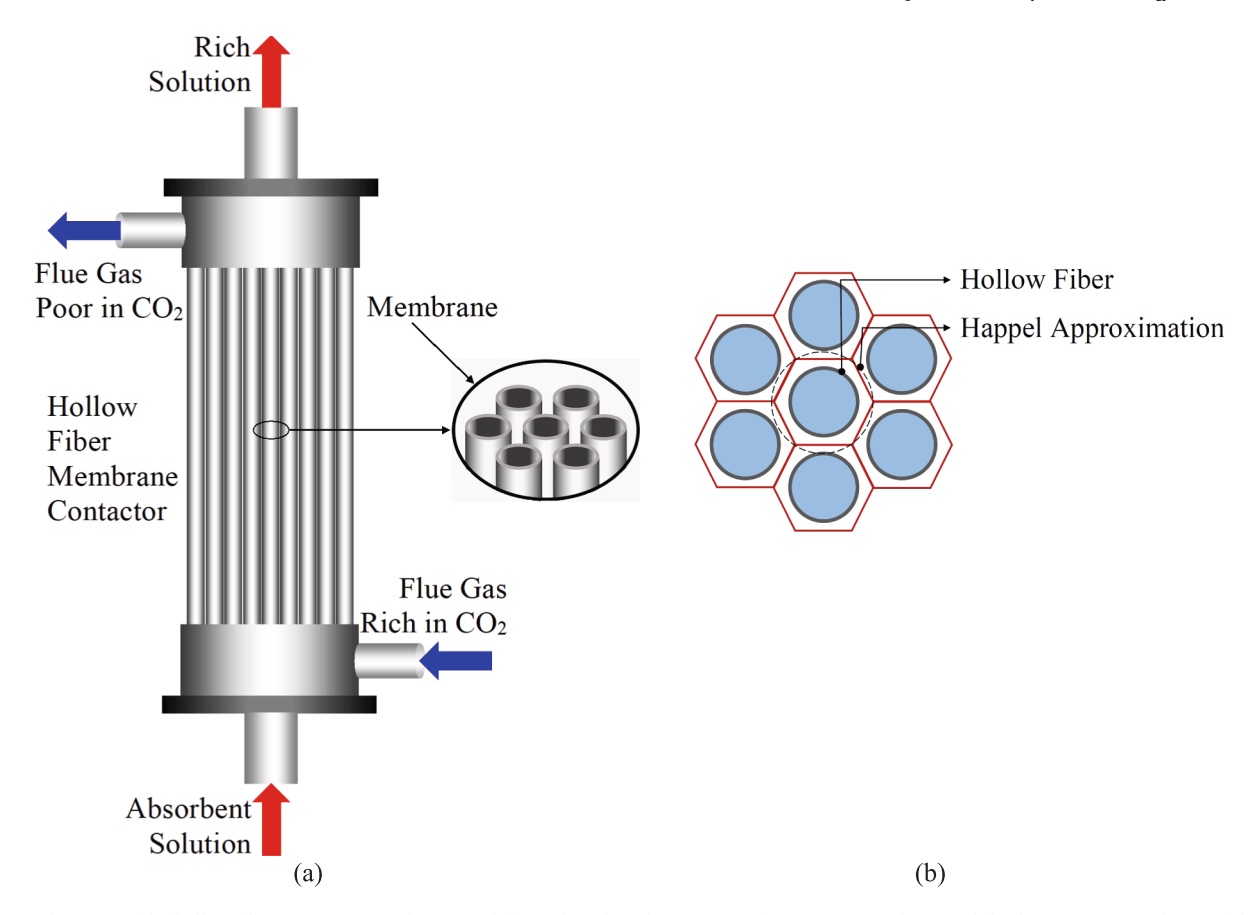


Fig. 1. (a) Schematic of the hollow fiber contactor membrane stack for carbon dioxide separation from sour natural gas, and (b) the cross-sectional area of the hollow fiber contactor membrane, approximated using the Happel model [33].

Table 1 System's geometric parameters[34].

Geometric parameters	Amount	Unit
Length of module	250	[mm]
Outer diameter	830	[µm]
Inner diameter	450	[µm]
Quantity of fibers	10	[-]
Effective length	175	[mm]

tube-tube system in which the radius of the outer tube is calculated based on Happel's model, as illustrated in Fig. 2. The wall of the inner tube is a porous membrane that is located between the gas and absorber.

Based on geometry symmetry, a two-dimensional symmetric mathematical model is developed for carbon dioxide separation from methane using the COMSOL software and the finite element numerical solution method. In this model, mass transfer and fluid equations are solved simultaneously. The membrane is modeled in dry and wet states, the absorbent can occupy the membrane voids completely or partially.

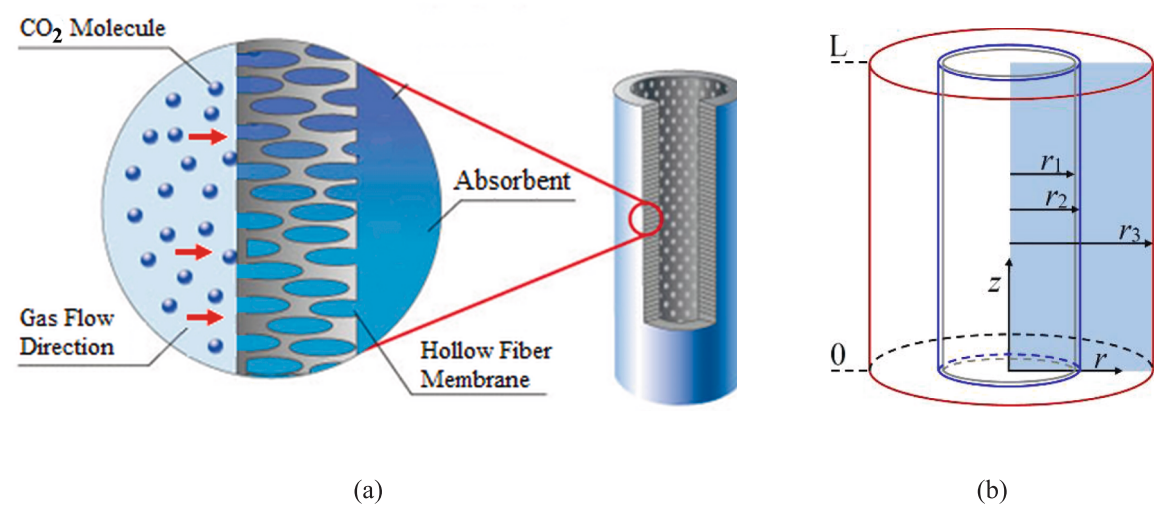


Fig. 2. (a) Membrane separation system for a wetted membrane and (b) two-dimensional representation of the contacting membrane and geometric parameters.

To simplify the numerical analysis, the following assumptions have been made:

- The membrane properties are considered uniform in all directions.
- Henry's law describes the equilibrium between the liquid and gas phases.
- The operating conditions of the process are assumed to be isothermal.
- The pores and voids of the membrane are uniform, and their density on the membrane surface is the same.
- Fick's law is employed for the diffusion and permeation of gas through the membrane.
- The behavior of the incoming gas mixture into the membrane module is considered ideal.
- The gas flow into the membrane module is assumed to be laminar, fully developed, and steady.
- Membrane deformation and swelling effects were neglected in the present simulations, assuming a rigid and dimensionally stable membrane structure throughout the process.

3. Governing equations

Mass and momentum conservation equations are applied to represent this process. The conservation of mass for all components in all membrane sections is [35]:

$$\nabla \bullet (-D_i C_i + C_i u) + \frac{\partial C_i}{\partial t} = R_i$$
 (1)

In Eq. (1), the first term on the left-hand-side corresponds to the mass transfer due to molecular diffusion, the second term represents convective mass transfer, the third term represents mass accumulation, and the term on the right-hand-side accounts for the reaction rates of the components per unit time and space. In variable C_i is the concentration of each component, D_i is the molecular diffusion coefficient of components, u is the fluid velocity, and u is the reaction rate of components in each section.

3.1. Mass conservation equation in the shell

Considering that no reactions occur in the shell, a steady-state process is assumed leading to a reduced general mass transfer Eq. (1) for CO₂:

$$D_{\text{CO}_2-\text{shell}} \left[\frac{\partial^2 C_{\text{CO}_2-\text{shell}}}{\partial r^2} + \frac{1}{r} \frac{\partial C_{\text{CO}_2-\text{shell}}}{\partial r} + \frac{\partial^2 C_{\text{CO}_2-\text{shell}}}{\partial z^2} \right] = V_{z-\text{shell}} \frac{\partial C_{\text{CO}_2-\text{shell}}}{\partial z} \quad (2)$$

In Eq. (2), the Happel model with a free surface is used to analyze the velocity distribution in the shell [33]. Various articles have utilized this model to investigate the velocity distribution in the shell of hollow fiber membrane contactors. However, the flow in this section does not entirely conform to the Happel models. Nevertheless, based on the studies that were conducted, e.g., [33], this model can accurately predict the velocity distribution in the outer tube. The velocity distribution model for the free surface Happel in the shell is as follows [33]:

$$V_{z-shell} = 2u \left[1 - \left(\frac{r_2}{r_3} \right)^2 \right] \times \frac{(r/r_3)^2 - (r_2/r_3)^2 + 2ln(r_2/r)}{3 + (r_2/r_3)^4 - 4(r_2/r_3)^2 + 4ln(r_2/r_3)}$$
(3)

where u is the average velocity in the shell, r_3 is the radius of the free surface, and r_2 is the outer radius of the fiber. These parameters are illustrated in Fig. 2(b). The radius of the free surface is calculated based on the following:

$$r_3 = \left(\frac{1}{1-\varphi}\right)^{1/2} r_2 \tag{4}$$

Equation (5) is used to calculate void volume inside the module (φ) in the hollow fiber membrane:

$$1 - \varphi = \frac{m_2^2}{R^2} \tag{5}$$

where R represents the inner radius of the module, and n represents the number of fibers.

For wetted membranes, the absorbent fills the membrane voids; therefore, mass transfer equations differ depending on membrane type and degree of wetting. In Fig. 2, the membrane is completely wetted, also known as flooded, with the absorbent occupying all voids in the membrane. Fig. 3, by contrast, illustrates a partially wetted membrane.

3.2. Mass conservation equation in the membrane

As surface tension decreases, the absorbent can penetrate the membrane pores. Therefore, the membrane can have dry and wet sections. In the wetted section, only the absorbent fills the porosity of the membrane, and in the dry section, the pores are filled with gas, and then the mass conservation equation in dry and wet sections must be considered separately. In practical applications of membrane absorption, pore wetting does not occur uniformly; larger pores tend to become wetted first, followed by smaller ones as liquid pressure increases. In this model, however, the wetting process is not explicitly simulated. Instead, it is assumed that all membrane pores become fully wetted at a specific time, and the effect of this fully wetted condition on membrane performance is then analyzed.

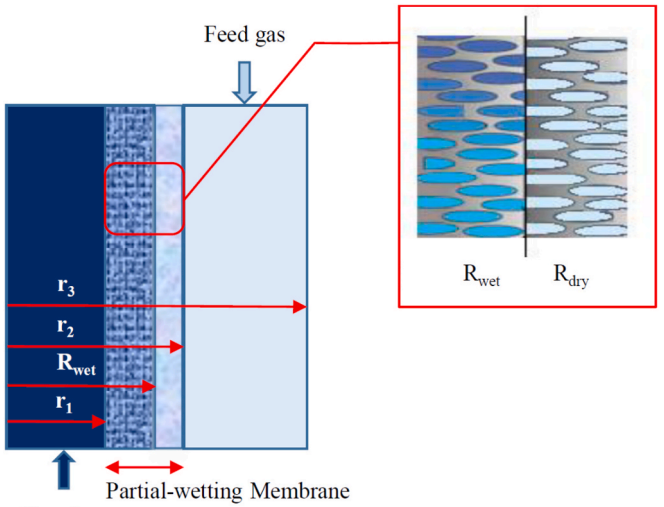
3.2.1. Non-wetting side

Assuming the pores are gas-filled, the dry section of the membrane is considered to consist solely of the gas phase. As shown in Fig. 3, the membrane thickness is assumed to be filled with gas equal to $R_{dry.}$ Therefore, the mass conservation equation in this section ($R_{wet} < r < r_2 - R_{wet}$) are as follows:

$$D_{i-g-m} \left[\frac{\partial^2 C_{i-g-m}}{\partial r^2} + \frac{1}{r} \frac{\partial C_{i-g-m}}{\partial r} + \frac{\partial^2 C_{i-g-m}}{\partial z^2} \right] = 0$$
 (6)

and the following boundary conditions are applied:

$$\begin{split} C_{CO_2-g-m} &= \frac{C_{CO_2-l-m}}{m_{CO_2}} & at & r = R_{wet} \\ C_{CO_2-g-m} &= C_{CO_2-shell} & at & r = r_2 \end{split} \tag{7}$$



Absorbent

Fig. 3. A two-dimensional schematic of a hollow fiber membrane contactor with a partially wetted membrane.

3.2.2. Wetting side

As illustrated in Fig. 3, it is assumed that a part of the membrane is occupied by absorbent. Therefore, the equation for this membrane section must be solved for gas permeation into MEA, incorporating the reaction term into the equation. The mass transfer process in the wetted section in the membrane ($r_3 < r_2 - r_3$) relies on solution-diffusion, where a reaction occurs after gas permeation into the absorbent that has occupied the membrane pores.

$$D_{i-CO_2-m} \left[\frac{\partial^2 C_{i-CO_2-m}}{\partial r^2} \frac{1}{r} \frac{\partial C_{i-CO_2-m}}{\partial r} \frac{\partial^2 C_{i-CO_2-m}}{\partial z} \right] + R_{i-CO_2-m} = 0$$
 (8)

Considering that the reaction is volumetric and occurs within the porous section of the membrane, the reaction rate is defined as follows:

$$R_{i-CO_2-m} = R_i \times \varepsilon \tag{9}$$

where ε represents the porosity of the membrane.

The boundary conditions are as follows:

$$\begin{array}{lll} C_{CO_2-l-m} = C_{CO_2-tube} & \text{at} & r = r_1 \\ C_{CO_2-l-m} = C_{CO_2-m} \times m_i & \text{at} & r = R_{wet} \end{array} \eqno(10)$$

where m_i is determined based on Henry's law as solubility of CO_2 absorbent.

3.3. Mass conservation equation in the tube side

In the tube section, a portion of the unreacted carbon dioxide from the wetted membrane region diffuses into the tube and reacts with the absorbent along the membrane length. The mass transfer equation for CO_2 in the tube, considering the effects of convective transport, molecular diffusion, and chemical reaction, is defined as follows:

$$D_{CO_2-tube} \left[\frac{\partial^2 C_{CO_2-tube}}{\partial r^2} + \frac{1}{r} \frac{\partial C_{CO_2-tube}}{\partial r} + \frac{\partial^2 C_{CO_2-tube}}{\partial z^2} \right]$$

$$= V_{z-tube} \frac{\partial C_{CO_2-tube}}{\partial z} + R_{i-CO_2-tube}$$
(11)

where $C_{CO2\text{-tube}}$, $D_{CO2\text{-tube}}$, and $R_{CO2\text{-tube}}$ are the CO_2 concentration in tube side, the diffusion coefficient of CO_2 in the absorbent, and the reaction rate of CO_2 with the absorbent, respectively.

Vz-tube is calculated based on the following equation:

$$V_{z-nibe} = 2\nu \left[1 - \left(\frac{r}{R_1} \right)^2 \right] \tag{12}$$

where v is the average velocity on the tube side. The boundary conditions in the tube side are:

$$C_{CO_2-tube}=0$$
 at $z=0$
$$C_{CO_2-l-m}=C_{CO_2-tube}$$
 at $r=r_1$
$$\frac{\partial C_{CO_2-tube}}{\partial r}=0$$
 at $r=0$
$$D_{CO_2-tube} \frac{\partial C_{CO_2-tube}}{\partial r}=0$$
 at $z=L$

3.4. Chemical reaction of carbon dioxide with various absorbents

Three reactions occur for the reaction of CO₂ in aqueous solutions. One of them is related to the hydration of CO₂ as follows,

$$CO_2 + H_2O \leftrightarrow HCO_3^- + H^+ \qquad k = 0.026s^{-1} (T = 25^{\circ}C)$$
 (14)

Due to its reaction rate constant being insignificant, this reaction is usually neglected [36].

Another reaction is producing bicarbonate according to the following reaction:

$$CO_2 + OH^- \leftrightarrow HCO_2^-$$
 (15)

Carbon dioxide reacts with a hydroxyl ion. The reaction is fast, but it requires hydroxyl ions.

The bicarbonate production reaction is represented by Equation (15), which is a relatively fast reaction [36]. This reaction is considered for all absorbents. Therefore, the overall reaction rate equation for each absorbent is:

$$r_{\text{overall}} = r_{\text{CO}_2-\text{absorbent}} + r_{\text{CO}_2-\text{OH}^-} \tag{16}$$

Table 2 presents the reaction rate of carbon dioxide with various absorbents and the formation of bicarbonates. The reaction rate of carbon dioxide with hydroxyl ions is very low compared to other reactions.

The required data for solving the momentum conservation equation in COMSOL include the density and viscosity of the fluids. Since pressure variations along the membrane are insignificant, and the model assumes isothermal conditions, absorbent's physical properties are assumed constant (Table 3).

The required data for solving the mass transfer equation includes the mass transfer coefficient and Henry's law constant. Considering isothermal conditions, these values are assumed constant as presented in Table 4

3.5. Penetration pressure

In the gas-liquid hollow fiber membrane contactor process, the dry mode occurs when the membrane pores are filled with gas, the gas separation efficiency is higher than when it is filled with liquid (wet mode) because gas passes through the membrane in the dry mode faster than in the wet mode. Therefore, it is better to avoid wetting of the membrane, which is the function of pressure difference between liquid in tube and gas in the pores of the membrane. For a dry membrane, the pressure difference needs to be lower than the liquid penetration pressure. Penetration pressure [43] is calculated with the following equation:

$$\Delta P = \frac{-2\sigma\cos\theta}{r_n} \tag{17}$$

where P, σ , θ , and r_p represent penetration pressure in MPa, liquid's surface tension in N/m, contact angle (degree) between the fluid and the pore of the membrane, and the membrane pore radius in meter, respectively. The values of σ and θ for water and a PVDF membrane are 72.8 mN/m and 100° , respectively. Therefore, based on Equation (17), the wetting pressure for this membrane is 0.126 MPa. The amounts of σ and θ between 2 M MEA solution and PVDF membrane are 67.3 mN/m and 28.5° [44]. Based on Equation (17), P for a 2 M MEA solution and a PVDF membrane is equal to 0.094 MPa. Hence, the possibility of wetting the PVDF membrane with MEA is higher than for water.

There is no experimental data for TEA and PZ absorbents. Thus, it is assumed that the possibility of TEA and PZ wetting the PVDF membrane is equal to MEA, this assumption is used to investigate the effect of the type of absorbent on the $\rm CO_2$ separation efficiency. As aqueous solutions are used to prevent water penetration in the membrane pore, the

Table 2
Reaction rates of carbon dioxide and different solutions as absorbent.

Absorbent	Reaction Rate	Reference
OH ⁻	$-(10^{13.635-\frac{2895}{T}})C_{CO_2}C_{OH^-}$	[36]
PZ [C ₄ H ₁₀ N ₂]	$-4.49 \times 10^{12} exp \left(-\frac{5712}{T}\right) C_{CO_2} C_{PZ}$	[37]
MEA [C ₂ H ₇ NO]	$-(10^{10.99-\frac{2152}{T}})10^{-3}C_{CO_2}C_{MEA}$	[38]
TEA [C ₆ H ₁₅ NO ₃]	$-4.52\times10^4 exp\bigg(-\frac{2688}{T}\bigg)C_{CO_2}C_{TEA}$	[39]

Table 3Properties of the absorbents.

Absorbent	MEA	PZ	TEA
Boiling Point [K]	443	416	608
Density at 298 K [g•cm ⁻³]	1.01	1.10	1.12
Flash Point [K]	366	360	458
Molar Weight [g∙mol ⁻¹]	61.08	86.13	149.19
Surface Tension at 298 K [g•s ⁻²]	48.89	70.20	48.90

Table 4Diffusion coefficient and Henry's law constant for carbon dioxide in various absorbents.

Parameter	Value	Reference
D _{CO2-shell}	$1.8 \times 10^{-5} \ [\text{m}^2 \bullet \text{s}^{-1}]$	[40]
$D_{CO2-membrane}$	$DCO_2 - shell (\varepsilon/\tau)[m^2 \bullet s^{-1}]$	[41]
$D_{MEA-tube}$	$9.3 \times 10^{-10} [\text{m}^2 \bullet \text{s}^{-1}]$	[42]
$D_{CO2-MEA}$	$1.51 \times 10^{-9} \ [\text{m}^2 \bullet \text{s}^{-1}]$	
$m_{CO2-MEA}$	0.81	
$D_{TEA-tube}$	$7.11 \times 10^{-10} \ [\text{m}^2 \bullet \text{s}^{-1}]$	[43]
$D_{CO2-TEA}$	$1.95 \times 10^{-9} [\text{m}^2 \bullet \text{s}^{-1}]$	
$m_{CO2-TEA}$	0.60	
$D_{PZ-tube}$	$1.05 \times 10^{-9} \ [\text{m}^2 \cdot \text{s}^{-1}]$	[37]
D_{CO2-PZ}	$1.51 \times 10^{-9} \ [\text{m}^2 \bullet \text{s}^{-1}]$	
m_{CO2-PZ}	1.06	

pressure difference between the gas and liquid phases is kept less than zero in all tests.

4. Solution method

The transport of diluted species and laminar flow interfaces in COMSOL are used to solve the momentum and mass conservation equations within each region of the membrane contactor system, using the numerical solution method parallel direct sparse solver (PARDISO). This method is a high-performance solver that is the default direct solver in COMSOL Multiphysics for coupled PDEs. In this approach, the governing equations are discretized, forming a system of algebraic equations represented in matrix form as follows:

$$FP = S ag{18}$$

PARDISO, a direct solver, efficiently solves the linear system defined by matrices F (coefficient matrix), S (known source terms), and P (variable matrix) for modeling CO_2 separation in hollow fiber membrane contactors. Through LU factorization, PARDISO transforms F into a triangular matrix, ensuring numerically stable and accurate solutions. Its efficiency relies on the sparse structure of F, with few non-zero elements, reducing memory usage and computational time. We validated the solver's accuracy by comparing results with experimental CO_2 removal data and multiphysics simulations of membrane-absorbent interactions, achieving errors below 5 %. This approach enabled rapid sensitivity analysis, assessing the impact of membrane wettability (20 %–60 %) and absorbent kinetics (MEA, PZ, TEA) on CO_2 separation performance under realistic conditions, supporting optimization of industrial gas separation processes.

4.1. Model validation

As presented in Table 5, two different sets of experimental data are used to validate the numerical predictions. Atchariyawut et al. [44] employed water as a physical absorbent for CO_2 absorption by means of PVDF hollow fiber membrane contactors. A PVDF membrane is naturally hydrophobic. However, if the pressure difference between the liquid and gas streams exceeds the wetting pressure, Equation (14), the membrane will be wet. They conducted their experiment in the dry mode by controlling different pressures between gas and liquid streams. The mass transfer flux of CO_2 through the membrane has been compared with Atchariyawut et al.'s [44] experimental data in a dry mode in the membrane pores. As presented in Fig. 4, the numerical predictions for a PVDF membrane agree well with the previously published experimental data.

The mass transfer flux of carbon dioxide through the membrane is calculated from Equation (19):

$$J_{CO_2} = (Q_{in} \times C_{in} - Q_{out} \times C_{out}) \times 273.15 \times \frac{1000}{22.4 \times T_{gas} \times S}$$
(19)

where Q_{in} and Q_{out} are the inlet and outlet gas flow rates in the outer tube section, respectively. The variables C_{in} and C_{out} are the CO₂ concentrations at the inlet and outlet of the outer tube, T_{gas} is the gas temperature, and S is the interface area between the gas and liquid. At low water velocity, there is a small quantitative deviation between the model results and the experimental data.

Also, the numerical model and experimental results are compared for MEA chemical absorbent. As illustrated in Fig. 5(a), the model results align closely with the experimental data from Faiz and Al-Marzouqi [41] for $\rm CO_2$ concentration along the outer tube for monoethanolamine chemical absorbent. The maximum deviation between the predicted and

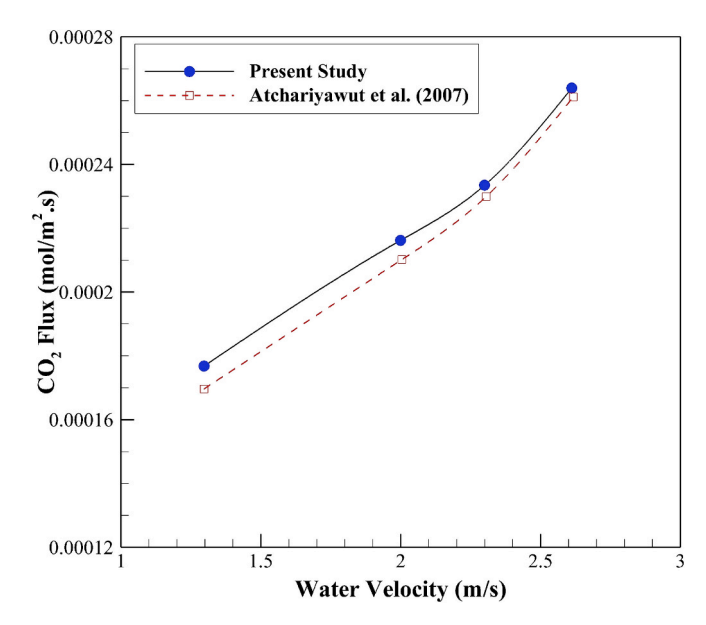
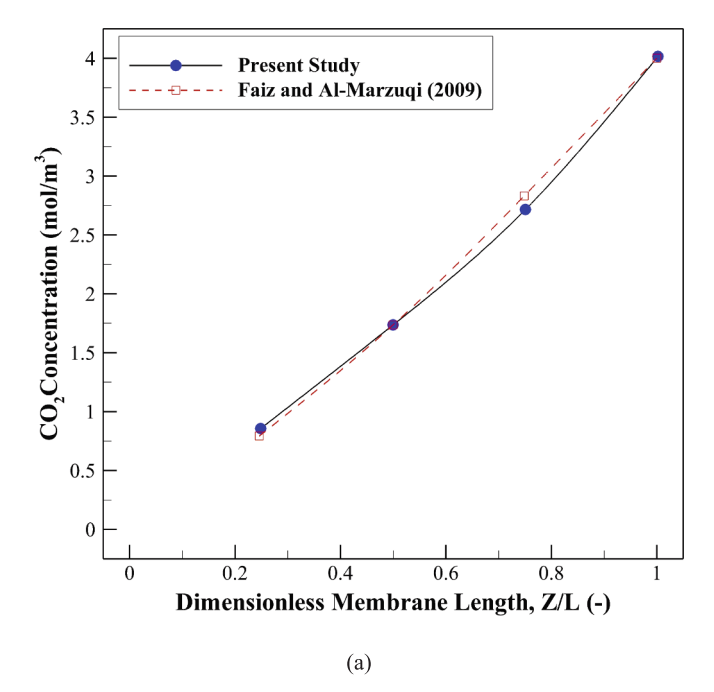


Fig. 4. Comparison of predicted carbon dioxide flux with experimental data [44] for membrane: PVDF, $CO_2:CH_4=20:80$, gas flow rate is equal to $200 \ (ml \bullet min^{-1})$.

Table 5Dimensions and properties of the membrane module used for model validation.

Module Type	Fiber Outer Diameter (mm)	Fiber Inner Diameter (mm)	Membrane Porosity	Tortuosity	Number of Fiber	Module Length (cm)	Reference
PVDF	0.3	0.22	0.40	2	3600	22	[41]
PVDF	1.0	0.65	0.75	4	35	27	[44]



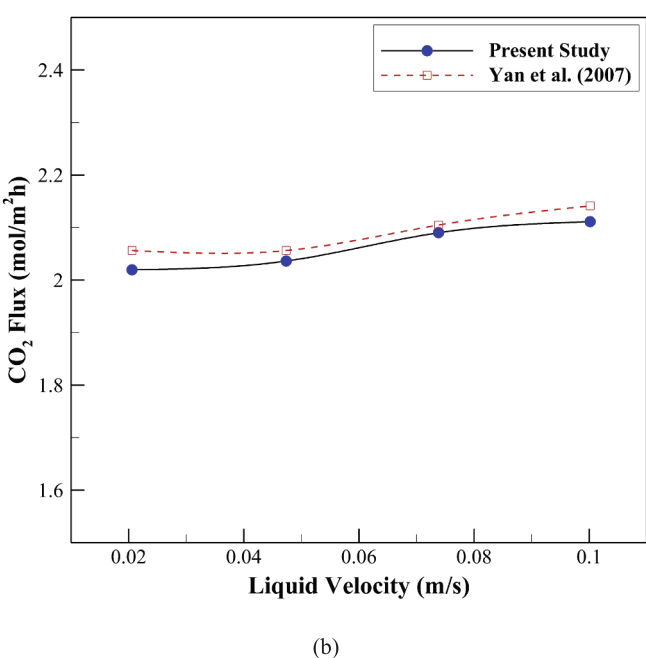


Fig. 5. (a) A comparison of the model and experimental data from [41] for the carbon dioxide concentration along the membrane at $V_{gas}=3.33~\text{m} \cdot \text{s}^{-1}$, $V_{MEA}=0.67~\text{m} \cdot \text{s}^{-1}$, $C_{MEA}=1000~\text{mol} \cdot \text{m}^{-3}$, gas feed: C_{CO2} inlet = 4 mol $\cdot \text{m}^{-3}$ and (b) Comparison between the modeled flux of CO_2 absorption and the experimental data of Yan et al. [45] ($V_{gas}=2.11~\text{m} \cdot \text{s}^{-1}$; $T_{gas}=298~\text{K}$, CO_2 volume fraction in feed gas is 14 %).

experimental values is less than 5 %, with the normalized root mean square error (nRMSE) calculated at 2.82 %. To ensure the accuracy of the model, the experimental data reported by Yan et al. [45] for $\rm CO_2$ absorption using MEA were simulated. The comparison between the model predictions and the experimental data is illustrated in Fig. 5(b). The model demonstrates good agreement with the experimental results for the prescribed conditions. This demonstrates the reliability of the model in predicting $\rm CO_2$ concentration. The specifications of the hollow fiber membrane from the experimental data are presented in Table 5.

5. Results and discussion

5.1. Effect of membrane wetting on CO₂ separation efficiency

Carbon dioxide removal efficiency was investigated under three membrane conditions: dry, 20 % wetted, and 60 % wetted. These scenarios were selected to analyze the impact of the membrane's physical and chemical conditions of absorbent on the process performance. As illustrated in Fig. 6, using MEA as the absorbent, the dry membrane achieves $100 \% \text{ CO}_2$ removal across all tested gas velocities, indicating optimal performance under dry conditions. However, when the membrane is partially wetted—specifically at 20 % of its width—the efficiency of CO_2 removal significantly declines.

Table 6 presents the percentage reduction in CO_2 separation efficiency compared to the dry membrane across different gas velocities and wetting degrees. At the lowest investigated gas velocity, 20 % membrane wetting leads to only an 11 % reduction in performance. In contrast, at the highest gas velocity of 3.3 m/s, the efficiency decreases dramatically by 67 %. This trend suggests that under high-flow conditions, partial wetting considerably impairs membrane performance. When the wetting ratio is increased to 60 % of the membrane width, the separation efficiency further declines by approximately 70 %, even at low gas velocities.

5.2. Explanation of performance Degradation in wetted membranes

The significant reduction in separation efficiency under wetted conditions can be attributed to changes in the mass transfer mechanisms within the membrane. In a dry membrane, the pores are filled with gas, and the dominant resistance is related to the diffusion of ${\rm CO_2}$ through the pores toward the absorbent interface, where the reaction occurs efficiently.

In contrast, in wetted membranes, the pores are occupied by liquid absorbent. This drastically increases the mass transfer resistance because CO_2 must now diffuse through a liquid phase with a much lower diffusion coefficient than gas. As a result, the transfer rate of CO_2 is reduced, leading to lower absorption efficiency.

Fig. 7 demonstrates the CO_2 concentration profiles along the membrane for both dry and 20 % wetted cases. The gradient of CO_2 concentration across the membrane is noticeably steeper in the wetted case,

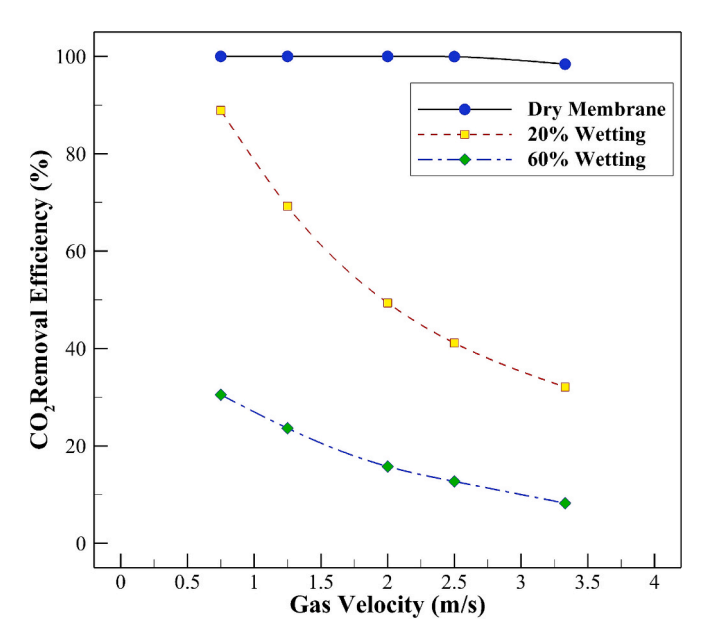


Fig. 6. Gas velocity effect on the carbon dioxide separation efficiency along the membrane in dry and wetted membranes at $V_{MEA}=0.67~\text{m} \cdot \text{s}^{-1}$, $C_{MEA}=1000~\text{mol} \cdot \text{m}^{-3}$, gas feed: C_{CO2} inlet = 4 mol \cdot m⁻³.

Table 6
Percentage decrease in carbon dioxide removal efficiency in the wet mode compared to the dry membrane at different gas velocities.

Velocity (m•s ⁻¹)	Wetting			
	20 %	30 %	40 %	60 %
0.75	11.082	19.630	28.501	69.501
1.25	30.784	37.875	43.391	76.391
2.00	50.623	57.926	63.224	84.226
2.50	58.845	67.066	74.294	87.302
3.33	67.396	77.648	84.519	91.632

indicating slower transport and increased accumulation near the membrane surface. As time progresses, the membrane pores become saturated with absorbent, further increasing resistance and reducing efficiency.

5.3. Absorbent behavior and concentration dynamics in wetted regions

In addition to the increased mass transfer resistance, changes in the absorbent concentration also contribute to the reduced separation efficiency in wetted membranes. Fig. 8 presents contour plots of MEA concentration within both the membrane and tube regions under wetted conditions. Although theoretically, a wetted or partially wetted membrane could offer better contact between ${\rm CO_2}$ and the absorbent, practical limitations arise.

As CO_2 reacts with the MEA inside the membrane pores, the local absorbent concentration diminishes. Without the continuous replacement of fresh MEA or effective removal of reaction products, the system transitions into a solution-diffusion regime, which is far less efficient. In contrast, the dry membrane benefits from a continuous supply of fresh absorbent at the gas–liquid interface and rapid removal of the reaction product, maintaining high reaction rates and efficiency.

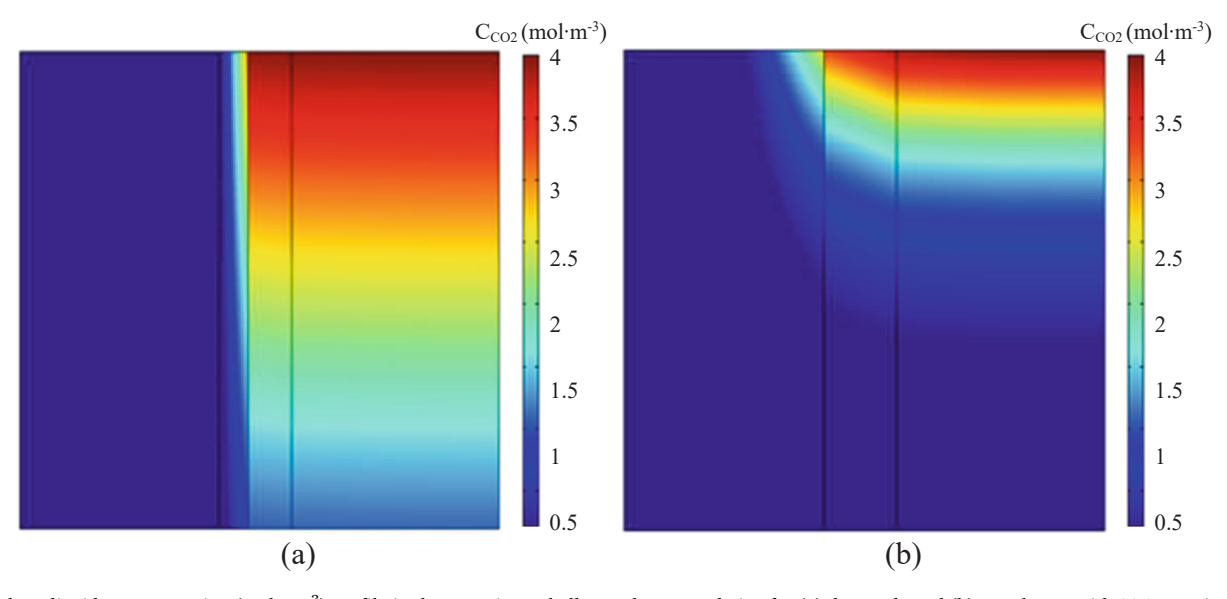


Fig. 7. Carbon dioxide concentration (mol \bullet m⁻³) profile in three sections: shell, membrane, and pipe for (a) dry mode and (b) membrane with 20 % wetting at V_{MEA} = 0.67 m \bullet s⁻¹, C_{MEA} = 1000 mol \bullet m⁻³, gas feed: C_{CO2} inlet = 4 mol \bullet m⁻³. (Horizontal axis is the width and the vertical axis is the length.).

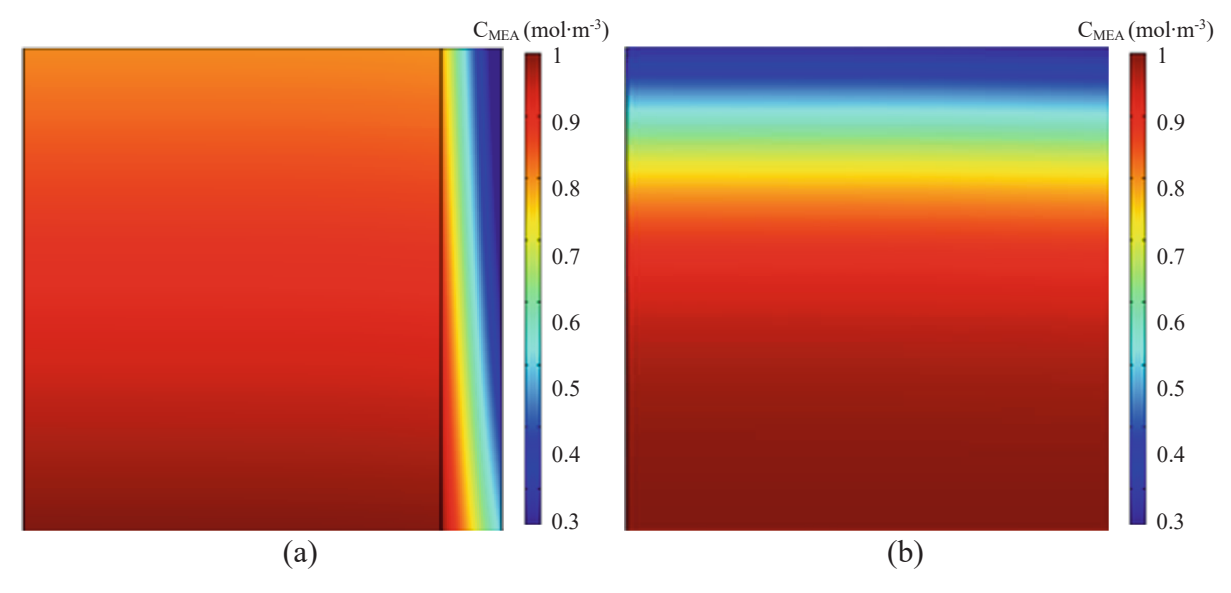
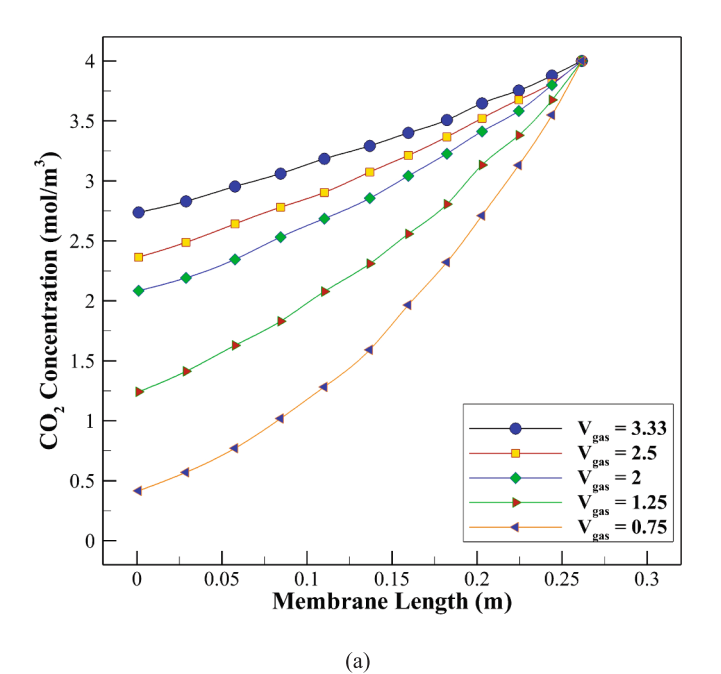


Fig. 8. (a) Absorbent concentration ($\times 1000$) profile in the tube region for the dry membrane case and (b) Absorbent concentration ($\times 1000$) variations in the wetted regions of the membrane and the tube at $V_{MEA} = 0.67 \text{ m} \cdot \text{s}^{-1}$, $C_{MEA} = 1000 \text{ mol} \cdot \text{m}^{-3}$, gas feed: C_{CO2} inlet = 4 mol \cdot m⁻³. (Horizontal axis is the width and the vertical axis is the length.).

This comparison confirms that a dry membrane not only minimizes resistance but also ensures better absorbent utilization, explaining its superior performance across all tested conditions.

5.4. Effects of gas velocity on the CO₂ concentration along the membrane

As illustrated in Fig. 9, a dry membrane's carbon dioxide removal efficiency is remarkably higher than when the membrane is wetted. The changes in carbon dioxide concentration in a dry membrane decrease sharply at all gas velocities. This is in contrast to the wetted membrane, although only 20 % of the membrane is considered wetted, the mass transfer resistance of carbon dioxide in the membrane substantially increases. Initially, a significant portion of the gas permeates the membrane and undergoes a reaction with the absorbent. However, due to the



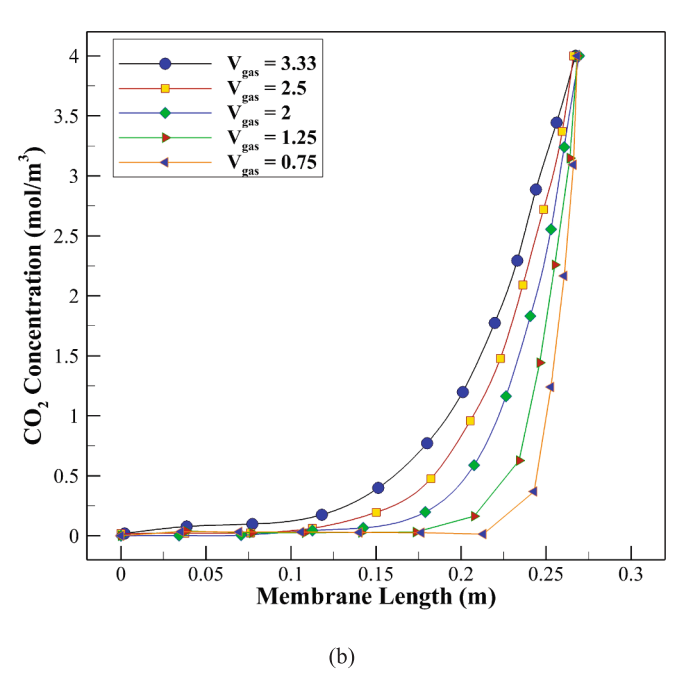


Fig. 9. The effect of gas velocity on the carbon dioxide concentration along the membrane for (a) a dry membrane and (b) a membrane with 20 % wetting at $V_{\text{MEA}}=0.67~\text{m}\,\text{es}^{-1}$, $C_{\text{MEA}}=1000~\text{mol}\,\text{em}^{-3}$, gas feed: C_{CO2} inlet = 4 mol $\,\text{em}^{-3}$.

limited absorbent within the membrane pores, the mass transfer mechanism shifts, leading to a significant increase in mass transfer resistance.

For an increase in gas velocity, the concentration difference between the outer tube and membrane sections increases, however, the mass transfer resistance intensifies due to the absorbent permeating into the membrane. Therefore, features such as the limited solubility of carbon dioxide in the absorbent and the low diffusion coefficient of carbon dioxide in the absorbent cause the removal efficiency to sharply decrease with increasing gas phase velocity. In contrast, at a distance of 0.15 m from the length of the membrane contactor for the dry membrane, as the gas flow velocity increases from 0.75 to 3.3 m/s, only a 7 % decrease in carbon dioxide removal efficiency is predicted. Therefore, the presented results indicate that membrane wetting considerably impacts gas removal efficiency, even at low wetting percentages of the membrane.

5.5. Effects of liquid velocity on CO₂ concentration along the membrane

Mass transfer resistance of the absorbent is an important parameter pertaining to separating carbon dioxide in membrane contactors. Increasing liquid velocity is one method to reduce mass transfer resistance in fluids. Convection mass transfer is increased by increasing fluid velocity, which causes a decrease in the mass transfer resistance. In a completely dry membrane, as illustrated in Fig. 10 for an absorbent velocity is 0.33 m/s, the carbon dioxide concentration only decreases sharply in the initial 40 % of the membrane length. However, as it approaches the outlet, the slope of the changes in carbon dioxide concentration diminishes. This could be attributed to 1) the reduction in carbon dioxide concentration within the shell, resulting in a decrease in the concentration gradient between the shell and tube sections, and 2) the decrease in the available absorbent concentration for reacting with carbon dioxide in the 60 % end of the membrane.

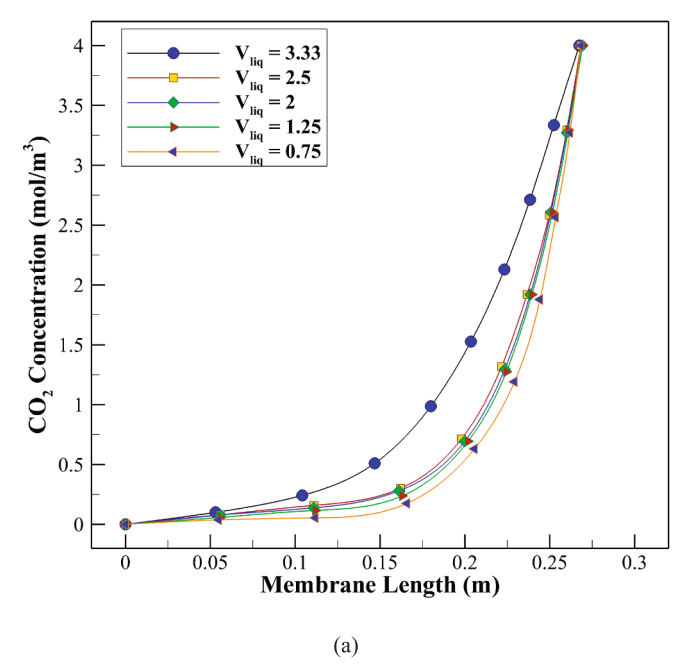
As absorbent velocity increases from 0.33 to 1.2 m/s, carbon dioxide is wholly separated in 60 % of the initial membrane length. However, with an increase in absorbent velocity from 1.2 to 2.7 m/s, the effect of absorbent velocity on changes in carbon dioxide concentration becomes insignificant. This implies that when the absorbent velocity is equal to 1.2 m/s, the speed of the absorbent is no longer the controlling factor of mass transfer resistance, and other resistances within the system are primary. In contrast, for a membrane with 20 % wetting, the results differ significantly from a completely dry membrane. As illustrated in Fig. 10, the carbon dioxide concentration along the membrane does not alter significantly with changes in absorbent velocity.

As illustrated in Fig. 11, the efficiency is 100 % for a dry membrane at all investigated absorbent velocities. According to Fig. 11, only the required membrane length changes to achieve 100 % efficiency. However, for a membrane with 20 % wetting at all investigated velocities, the efficiency is less than 40 %. As the velocity increases from 0.33 to 1.2 m/s, only 5 % improvement in carbon dioxide separation efficiency is achieved. No significant change in efficiency with an increase in velocity from 1.2 to 2.7 m/s. This result indicates that the primary resistance within the wetted membrane is the wetting itself, which significantly reduces mass transfer as the membrane pores become occupied by absorbent.

5.6. Effect of absorbent type on CO_2 removal efficiency in wetted and dry membranes

Numerical predictions for two absorbents, PZ and TEA, are presented in this section. As presented in Table 3, the reaction rate of PZ with carbon dioxide is significantly greater than that of the other absorbents, and the reaction rate of TEA with carbon dioxide is the lowest among all absorbents. However, for a dry membrane the absorbent type is not critical, and the removal efficiency is close to 100 % for all predicted flow rates for the three absorbents (Fig. 12).

The results predict that the absorbent type is important for wetted



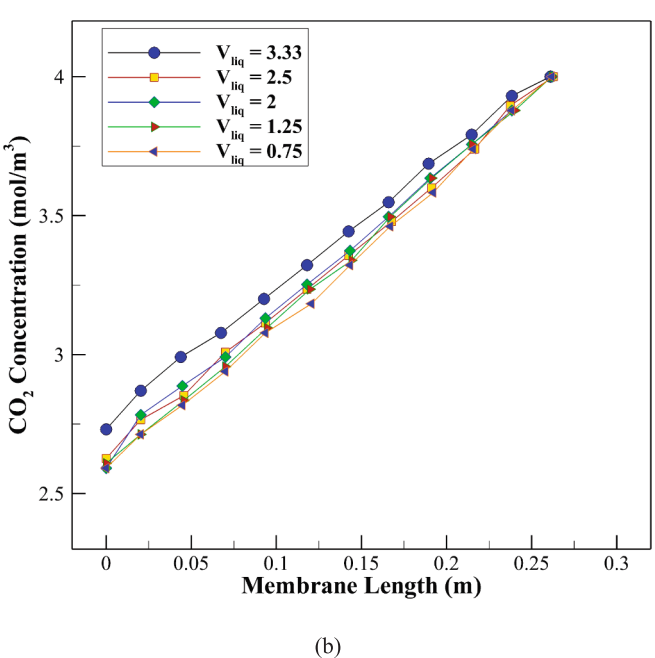


Fig. 10. Liquid velocity effect on carbon dioxide concentration along the membrane for (a) a dry membrane and (b) a membrane with 20 % wetting at $V_{gas}=0.33~\text{m} \cdot \text{s}^{-1}$, $C_{MEA}=1000~\text{mol} \cdot \text{m}^{-3}$, gas feed: C_{CO2} inlet = 4 mol $\cdot \text{m}^{-3}$.

membranes. Using the PZ absorbent (even with a 20 % wetted membrane), the removal efficiency achieves close to 100 % for gas flow rates ranging from 0.75 to 1.2 m/s. This is due to the significantly higher reaction rate of PZ with carbon dioxide compared to the other absorbents. The reaction rate of PZ is 500 times greater than that of MEA and 1000 times greater than that of TEA with carbon dioxide. Consequently, even though the membrane is filled with liquid PZ absorbent, the reaction rate and the quantity of moles of CO_2 involved in the reaction are considerable. At low gas flow rates, there is a balance between the oxygen diffusing into the membrane and the reaction rate of CO_2 with the absorbent. Therefore, any carbon dioxide entering the membrane pores reacts under steady-state conditions. However, as the gas velocity increases, due to the increased gas transfer rate to the membrane and the saturation of the absorbent inside the membrane pores, all the carbon

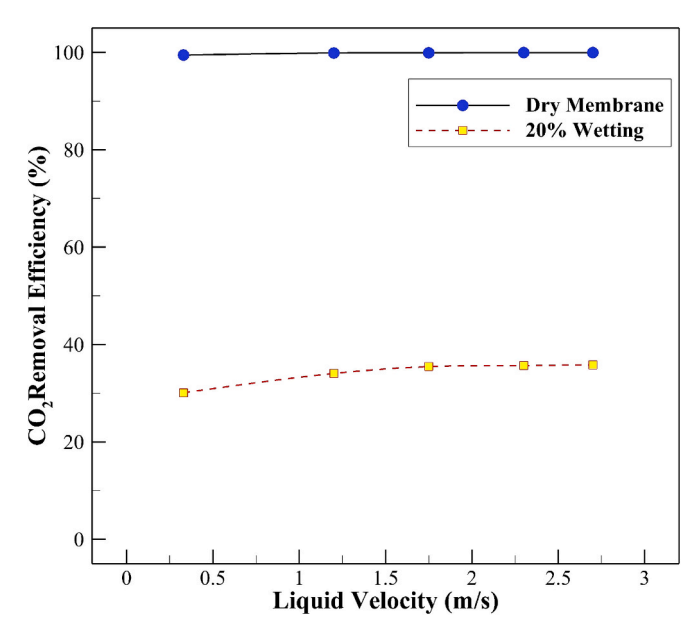


Fig. 11. Carbon dioxide removal efficiency with liquid velocity for dry and 20 % wetted membrane at $Vgas = 0.33 \text{ m} \cdot \text{s}^{-1}$, $C_{MEA} = 1000 \text{ mol} \cdot \text{m}^{-3}$, gas feed: C_{CO2} inlet $= 4 \text{ mol} \cdot \text{m}^{-3}$.

dioxide permeates into the membrane, unable to be dissolved and reacted by the absorbent. The increase in gas velocity significantly reduces the removal efficiency.

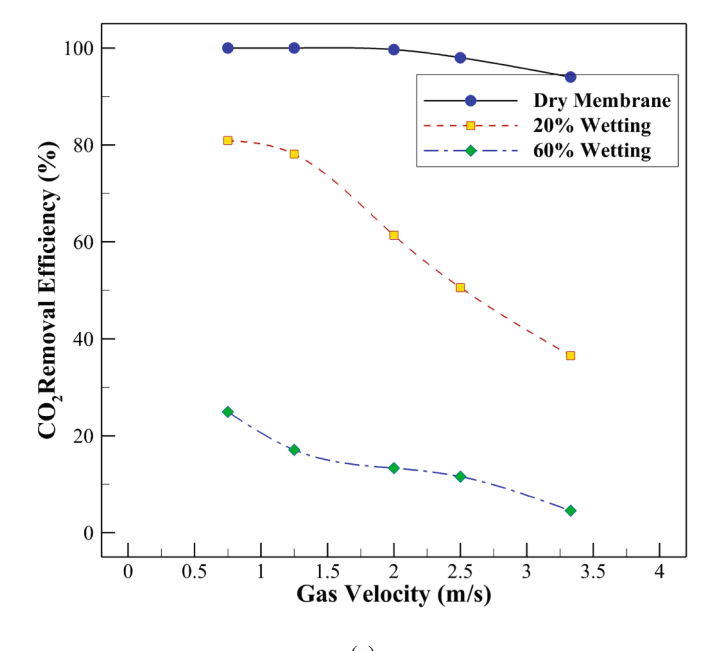
For the TEA absorbent, since the reaction rate is significantly lower than the other two absorbents, even at low gas flow rates, the removal efficiency decreases considerably compared with the dried membrane (Fig. 12). In high gas flow rates and 60 % wetting of the membrane, the removal efficiency reduces to less than 5 %.

As illustrated in Fig. 13, the efficiency is equal to 100 % for a dry membrane for all investigated absorbent velocities. However, for a membrane with 20 % wetting at all investigated velocities, the efficiency is approximately 60 %, which is higher than for the MEA absorbent. For an increase in velocity from 0.33 to 1.2 m/s, only about 10 % improvement in carbon dioxide separation efficiency is achieved. Furthermore, similar to an MEA absorbent, no significant change in efficiency is predicted for an increase in velocity from 1.2 to 2.7 m/s. Similar results indicate that the primary resistance within the wetted membrane is the wetting itself, which significantly reduces mass transfer as the membrane pores become occupied by absorbent.

Fig. 14 illustrates the predicted CO_2 removal efficiency (%) over time (in days) using different absorbents, including water, 2 M MEA, 2 M TEA, and 2 M PZ, for constant absorbent and gas velocities of 0.33 m/s. To clearly present the asymptotic behavior of extended time durations, a break is introduced in the X-axis after day 40. Beyond this break, the axis is labeled as "t", representing an arbitrary time greater than 40 days. This notation emphasizes the long-term trend without specifying an exact value, allowing for a generalized view of the asymptotic behavior of the system.

Based on reverse engineering using experimental data, it determined that a 43 % reduction in $\rm CO_2$ flux after 15 days corresponds to approximately 15 % membrane wetting. Assuming a linear increase in wetting, the membrane is predicted to reach 60 % wetting after approximately 60 days. At this level of wetting, the $\rm CO_2$ removal efficiencies for 2 M MEA, 2 M TEA, and 2 M PZ are 13 %, 12 %, and 21.5 %, respectively, demonstrating the superior performance of PZ due to its faster reaction kinetics with $\rm CO_2$. These findings emphasize the critical impact of progressive membrane wetting on long-term $\rm CO_2$ separation performance and offer guidance for absorbent selection in industrial applications.

Atchariyawut et al. [44] conducted long-term experiments using



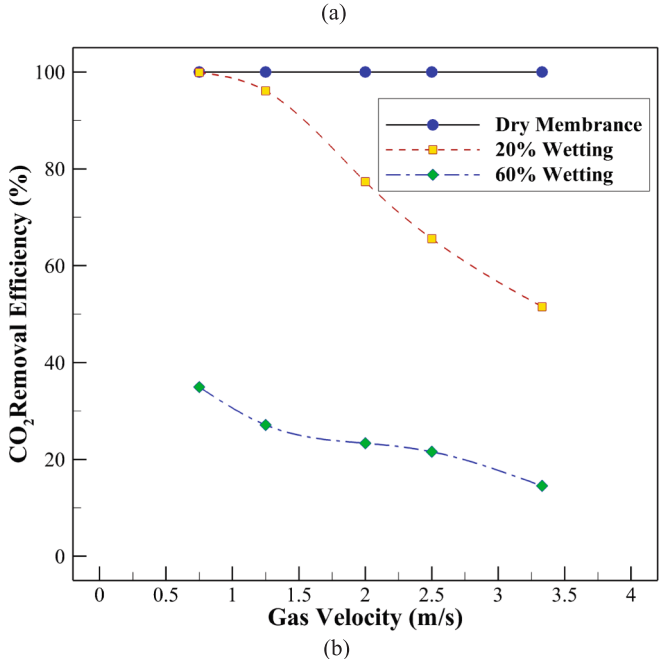


Fig. 12. Effect of chemical absorbent type on carbon dioxide removal efficiency at different gas flow rates for (a) TEA and (b) PZ absorbents at $V_{liquid} = 0.67~\text{m} \cdot \text{s}^{-1}$, $C_{MEA} = 1000~\text{mol} \cdot \text{m}^{-3}$, gas feed: C_{CO2} inlet = 4 mol \cdot m⁻³.

both water and 2 M MEA as absorbents and observed distinct trends in membrane wetting and CO_2 flux. Their results showed that for pure water, PVDF hydrophobic membranes exhibited no significant wetting over 15 days. In contrast, for 2 M MEA, the CO_2 flux decreased due to increased membrane wetting. Specifically, they reported approximately 15 % and 43 % reductions in CO_2 flux after 3 and 15 days, respectively [44], supporting the modeling assumptions of the present study.

Although the CO_2 removal efficiency using chemical absorbent decreases with time, it is more than when using water as an absorbent. If the membrane is wet with water after "t" time, the CO_2 removal efficiency will decrease, as shown in Table 7. As it can see after 10 % wetting the membrane with water, the CO_2 removal efficiency is close to zero. We have to consider that with increasing wetting at high gas velocity, the efficiency is not economical, and it is better to work at the high-pressure difference between gas and liquid streams, which is

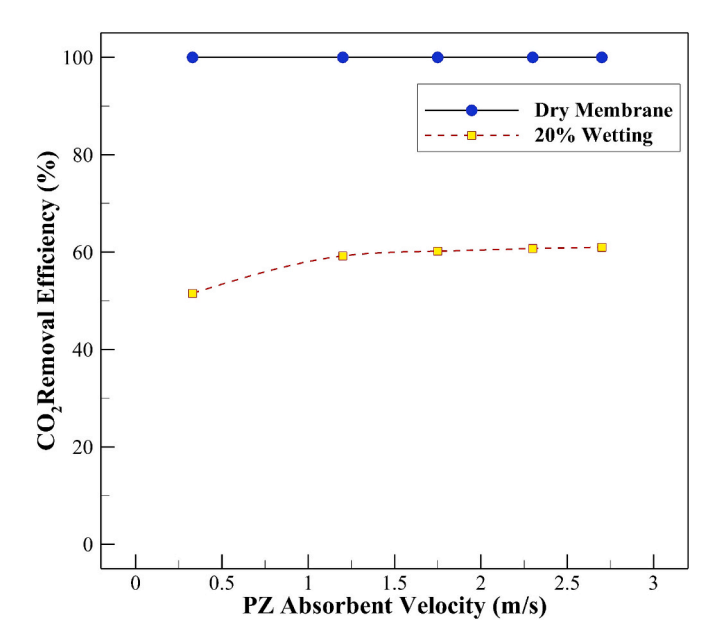


Fig. 13. The effect of the PZ absorbent velocity on the CO_2 absorbent removal efficiency at $V_{gas} = 0.33 \text{ m} \bullet \text{s}^{-1}$, $C_{MEA} = 1000 \text{ mol} \bullet \text{m}^{-3}$, gas feed: C_{CO2} inlet = $4 \text{ mol} \bullet \text{m}^{-3}$.

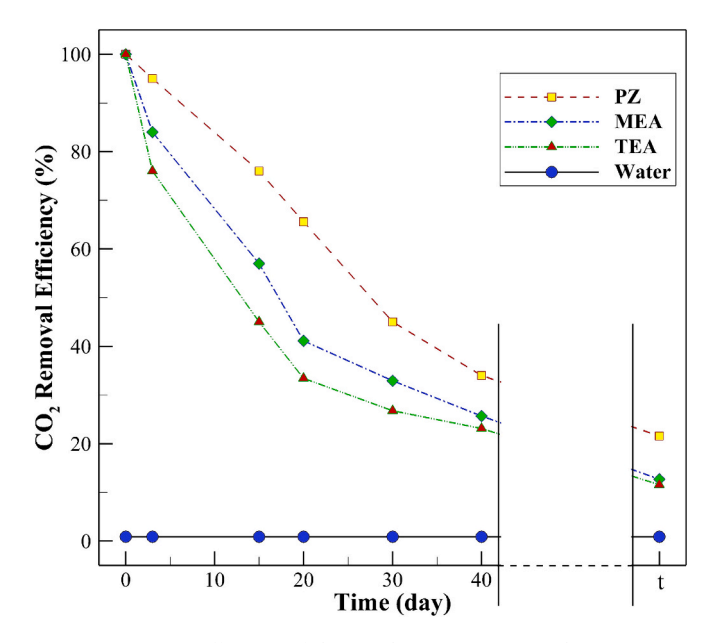


Fig. 14. Long-term efficiency of the membrane contactor in the process CO_2 removal using different absorbents content water, 2 M MEA, 2 M TEA, and 2 M PZ solutions as the absorbents (absorbent velocity: 0.33 m/s, gas velocity: 0.33 m/s, $C_{\text{MEA},PZ,TEA} = 2000 \text{ mol} \bullet \text{m}^{-3}$, gas feed: C_{CO2} inlet = 4 mol \bullet m⁻³.).

Table 7The CO₂ removal efficiency by water as the absorbent.

Water ${ m CO_2}$ Removal Efficiency				
Gas Velocity (m/s)	Dry Mode	20 % Wetting Mode		
0.75	1.865	0.868		
1.25	1.363	0.522		
2.00	1.028	0.327		
2.50	0.899	0.261		
3.33	0.761	0.198		

considerably lower than penetrating pressure.

6. Conclusions

In this paper, the effects of wetting of membrane on the CO_2 separation performance were investigated. The results show that:

- 1. When the membrane was 20 % wetted using MEA as the absorbent, there was only an 11 % decrease in CO_2 removal efficiency compared to a dry membrane. However, when the gas velocity increased to 3.3 m/s, the efficiency dropped to 67 %, indicating that the membrane did not maintain sufficient separation performance for these conditions. As the membrane wetting increased to 60 %, the efficiency further declined—reaching approximately 30 % at the lowest examined gas velocity and falling below 10 % at the highest velocity. These results suggested that such a degree of wetting caused the process to be economically unviable.
- 2. Membrane wettability negatively affected the performance of hollow fiber membrane contactors in the CO₂ gas separation process. The results predicted that with 20 % wetting of the membrane, the efficiency of CO₂ separation was reduced significantly.
- 3. Typically, the type of absorbent could significantly influence the removal efficiency. However, in our specific conditions, in the case of dried membranes, the chemical reaction between the absorbent and the permeated gas was extremely fast compared to the gas flow rate. As a result, the absorbent surface sites were not a limiting factor, and near-complete removal (~ 100 %) was predicted with all three types of chemical absorbents tested.
- 4. In the case of wetted membranes, the absorbent type was essential, and it had a remarkable impact on the efficiency. The reaction rate between ${\rm CO_2}$ and absorbent was important. The reaction rate of PZ was higher than other absorption and reaction rate of TEA was lower. The results predicted that in the case of wetted membranes, the lowest efficiency was reached with TEA, and the highest was reached with PZ.

It can be concluded that over time, most membranes exhibited minimal wettability. Therefore, the type of absorbent in the separation process was a critical parameter, and optimizing the process conditions when a portion of the membrane was wetted is significant.

To strengthen the practical relevance of this study, future work will focus on conducting experimental validation of the numerical predictions. This will include testing membrane performance for varying degrees of wettability and gas velocities using different chemical absorbents. Such experimental studies will confirm the reliability of the model and provide further insights into the operational feasibility and optimization of hollow fiber membrane contactors for $\rm CO_2$ Separation in real-world applications.

CRediT authorship contribution statement

Hamed Rahnema: Writing – original draft, Methodology, Conceptualization. Amin Etminan: Writing – review & editing, Writing – original draft, Visualization, Supervision, Project administration, Investigation, Formal analysis. Sara Barati: Writing – review & editing, Writing – original draft, Validation, Software, Investigation, Formal analysis, Data curation, Conceptualization. Kevin Pope: Writing – review & editing, Supervision, Project administration.

Declaration of competing interest

The authors declare that they have no known competing financial interests or personal relationships that could have appeared to influence the work reported in this paper.

Data availability

Data will be made available on request.

References

- [1] Y.S. Kashtan, M. Nicholson, C. Finnegan, Z. Ouyang, E.D. Lebel, D.R. Michanowicz, S.B.C. Shonkoff, R.B. Jackson, Gas and propane combustion from stoves emits benzene and increases indoor air pollution, Environ. Sci. Technol. 57 (26) (2023) 9653–9663, https://doi.org/10.1021/acs.est.2c09289.
- [2] S. Qazi, L. Gómez-Coma, J. Albo, S. Druon-Bocquet, A. Irabien, J. Sanchez-Marcano, CO₂ capture in a hollow fiber membrane contactor coupled with ionic liquid: Influence of membrane wetting and process parameters, Sep. Purif. Technol. 233 (2020) 115986, https://doi.org/10.1016/j.seppur.2019.115986.
- [3] S. Barati, B. Khoshandam, M.M. Ghazi, An investigation of channel blockage effects on hydrogen mass transfer in a proton exchange membrane fuel cell with various geometries and optimization by response surface methodology, Int. J. Hydrogen Energy 43 (48) (2018) 21928–21939, https://doi.org/10.1016/j. iihydene.2018.10.032.
- [4] S. Barati, M.M. Ghazi, B. Khoshandam, Study of effective parameters for the polarization characterization of PEMFCs sensitivity analysis and numerical simulation, Korean J. Chem. Eng. 36 (2019) 146–156, https://doi.org/10.1007/ s11814-018-0178-6.
- [5] X. Zhang, R. Zeng, K. Mu, X. Liu, X. Sun, H. Li, Exergetic and exergoeconomic evaluation of co-firing biomass gas with natural gas in CCHP system integrated with ground source heat pump, Energ. Conver. Manage. 180 (2019) 622–640, https://doi.org/10.1016/ji.enconman.2018.11.009.
- [6] H.Y. Zhang, R. Wang, D.T. Liang, J.H. Tay, Theoretical and experimental studies of membrane wetting in the membrane gas–liquid contacting process for CO₂ absorption, J. Membr. Sci. 308 (1–2) (2008) 162–170, https://doi.org/10.1016/j. memsci.2007.09.050.
- [7] A. Almoslh, F. Alobaid, C. Heinze, B. Epple, Comparison of equilibrium-stage and rate-based models of a packed column for tar absorption using vegetable oil, Appl. Sci. 10 (7) (2020) 2362, https://doi.org/10.3390/app10072362.
- [8] M. Biermann, H. Ali, M. Sundqvist, M. Larsson, F. Normann, F. Johnsson, Excess heat-driven carbon capture at an integrated steel mill–Considerations for capture cost optimization, Int. J. Greenhouse Gas Control 91 (2019) 102833, https://doi. org/10.1016/j.ijggc.2019.102833.
- [9] H. Wasajja, R.E. Lindeboom, J.B. van Lier, P.V. Aravind, Techno-economic review of biogas cleaning technologies for small scale off-grid solid oxide fuel cell applications, Fuel Process. Technol. 197 (2020) 106215, https://doi.org/10.1016/ if/jurge. 2019.106215
- [10] A. Jareteg, D. Maggiolo, S. Sasic, H. Ström, Finite-volume method for industrial-scale temperature-swing adsorption simulations, Comput. Chem. Eng. 138 (2020) 106852, https://doi.org/10.1016/j.compchemeng.2020.106852.
- [11] Y. Han, W.W. Ho, Design of amine-containing CO₂-selective membrane process for carbon capture from flue gas, Ind. Eng. Chem. Res. 59 (12) (2019) 5340–5350, https://doi.org/10.1021/acs.jecr.9b04839.
- [12] C.A. Scholes, Pilot plants of membrane technology in industry: challenges and key learnings, Front. Chem. Sci. Eng. 14 (3) (2020) 305–316, https://doi.org/10.1007/ s11705-019-1860-x.
- [13] M.H. El-Naas, M. Al-Marzouqi, S.A. Marzouk, N. Abdullatif, Evaluation of the removal of $\rm CO_2$ using membrane contactors: membrane wettability, J. Membr. Sci. 350 (1–2) (2010) 410–416, https://doi.org/10.1016/j.memsci.2010.01.018.
- [14] S. Hwang, W.S. Chi, S.J. Lee, S.H. Im, J.H. Kim, J. Kim, Hollow ZIF-8 nanoparticles improve the permeability of mixed matrix membranes for CO₂/CH₄ gas separation, J. Membr. Sci. 480 (2015) 11–19, https://doi.org/10.1016/j.memsci.2015.01.038.
- [15] A. Köhler, D. Pallarès, F. Johnsson, Modeling axial mixing of fuel particles in the dense region of a fluidized bed, Energy Fuel 34 (3) (2020) 3294–3304, https://doi. org/10.1021/acs.energyfuels.9b04194.
- [16] J.L. Li, B.H. Chen, Review of CO₂ absorption using chemical solvents in hollow fiber membrane contactors, Sep. Purif. Technol. 41 (2) (2005) 109–122, https:// doi.org/10.1016/j.seppur.2004.09.008.
- [17] O.G. Nik, X.Y. Chen, S. Kaliaguine, Functionalized metal organic framework-polyimide mixed matrix membranes for CO₂/CH₄ separation, J. Membr. Sci. 413–414 (2012) 48–61, https://doi.org/10.1016/j.memsci.2012.04.003.
- [18] H. Abdolahi-Mansoorkhani, S. Seddighi, CO₂ capture by modified hollow fiber membrane contactor: Numerical study on membrane structure and membrane wettability, Fuel Process. Technol. 209 (2020) 106530, https://doi.org/10.1016/j. fuproc.2020.106530.
- [19] H. Abdolahi-Mansoorkhani, S. Seddighi, H₂S and CO₂ capture from gaseous fuels using nanoparticle membrane, Energy 168 (2019) 847–857, https://doi.org/ 10.1016/j.energy.2018.11.117
- [20] M.H. Ibrahim, M.H. El-Naas, Z. Zhang, B. Van der Bruggen, CO₂ capture using hollow fiber membranes: a review of membrane wetting, Energy Fuel 32 (2) (2018) 963–978, https://doi.org/10.1021/acs.energyfuels.7b03493.
- [21] Y. Xu, Y. Lin, N.G.P. Chew, C. Malde, R. Wang, Biocatalytic PVDF composite hollow fiber membranes for CO₂ removal in gas-liquid membrane contactor, J. Membr. Sci. 572 (2019) 532–544, https://doi.org/10.1016/j. memsci.2018.11.043.
- [22] M. Mehdipourghazi, S. Barati, F. Varaminian, Mathematical modeling and simulation of carbon dioxide stripping from water using hollow fiber membrane contactors, Chem. Eng. Process. 95 (2015) 159–164, https://doi.org/10.1016/j. cep.2015.06.006.

- [23] K. Motahari, S. Barati, T. Miri, Mathematical modelling and simulation of carbon dioxide absorption from N₂ using hollow fiber membrane contactor, Period. Polytech., Chem. Eng. 60 (4) (2016) 266–272, https://doi.org/10.3311/ PPrh 8689
- [24] M.H. Al-Marzouqi, M.H. El-Naas, S.A. Marzouk, M.A. Al-Zarooni, N. Abdullatif, R. Faiz, Modeling of CO₂ absorption in membrane contactors, Sep. Purif. Technol. 59 (3) (2008) 286–293, https://doi.org/10.1016/j.seppur.2007.06.020.
- [25] P.K.P. Senthil, K. Hogendoorn, P.H.M. Feron, G. Versteeg, New absorption liquids for the removal of CO₂ from dilute gas streams using mebrane contractors, Chem. Eng. Sci. 57 (9) (2002) 1639–1651, https://doi.org/10.1016/S0009-2509(02) 00041-6.
- [26] K. Simons, K. Nijmeijer, M. Wessling, Gas-liquid membrane contactors for CO₂ removal, J. Membr. Sci. 340 (1–2) (2009) 214–220, https://doi.org/10.1016/j.memsci.2009.05.035.
- [27] M. Saidi, CO₂ absorption intensification using novel DEAB amine-based nanofluids of CNT and SiO₂ in membrane contactor, Chemical Engineering and Processing-Process Intensification 149 (2020) 107848, https://doi.org/10.1016/j. cm.2020.107848
- [28] A.T. Nakhjiri, A. Heydarinasab, Computational simulation and theoretical modeling of CO₂ separation using EDA, PZEA and PS absorbents inside the hollow fiber membrane contactor, J. Ind. Eng. Chem. 78 (2019) 106–115, https://doi.org/ 10.1016/j.ijec.2019.06.031.
- [29] S. Gilassi, N. Rahmanian, CFD modelling of a hollow fibre membrane for CO₂ removal by aqueous amine solutions of MEA, DEA and MDEA, Int. J. Chem. React. Eng. 14 (1) (2016) 53–61, https://doi.org/10.1515/ijcre-2014-0142.
- [30] O. Hosseinkhani, A. Kargari, H. Sanaeepur, Facilitated transport of CO₂ through Co (II)-S-EPDM ionomer membrane, J. Membr. Sci. 469 (2014) 151–161, https://doi. org/10.1016/j.memsci.2014.06.021.
- [31] W. Rongwong, R. Jiraratananon, S. Atchariyawut, Experimental study on membrane wetting in gas-liquid membrane contacting process for CO₂ absorption by single and mixed absorbents, Sep. Purif. Technol. 69 (1) (2009) 118–125, https://doi.org/10.1016/j.seppur.2009.07.009.
- [32] R. Wang, H.Y. Zhang, P.H.M. Feron, D.T. Liang, Influence of membrane wetting on CO₂ capture in microporous hollow fiber membrane contactors, Sep. Purif. Technol. 46 (1–2) (2005) 33–40, https://doi.org/10.1016/j.seppur.2005.04.007.
- [33] J. Happel, Viscous flow relative to arrays of cylinders, AlChE J 5 (2) (1959) 174–177, https://doi.org/10.1002/aic.690050211.
- [34] M. Fosi-Kofal, A. Mustafa, A. Ismail, M. Rezaei-DashtArzhandi, T. Matsuura, PVDF/ CaCO₂ composite hollow fiber membrane for CO₂ absorption in gas-liquid

- membrane contactor, J. Nat. Gas Sci. Eng. 31 (2016) 428–436, https://doi.org/10.1016/j.ingse.2016.03.053.
- [35] Y.S. Kim, S.M. Yang, Absorption of carbon dioxide through hollow fiber membranes using various aqueous absorbents, Sep. Purif. Technol. 21 (1–2) (2000) 101–109, https://doi.org/10.1016/S1383-5866(00)00195-7.
- [36] B.R.W. Pinsent, L. Pearson, F.J.W. Roughton, The kinetics of combination of carbon dioxide with hydroxide ions, Trans. Faraday Soc. 52 (1956) 1512–1520, https:// doi.org/10.1039/TF9565201512.
- [37] S. Bishnoi, G.T. Rochelle, Absorption of carbon dioxide into aqueous piperazine: reaction kinetics, mass transfer and solubility, Chem. Eng. Sci. 55 (22) (2000) 5531–5543, https://doi.org/10.1016/S0009-2509(00)00182-2.
- [38] D. Barth, C. Tondre, J.J. Delpuech, Stopped-flow investigations of the reaction kinetics of carbon dioxide with some primary and secondary alkanolamines in aqueous solutions, Int. J. Chem. Kinet. 18 (4) (1986) 445–457, https://doi.org/ 10.1002/kin.550180404.
- [39] S.W. Park, B.S. Choi, J.W. Lee, Chemical absorption of carbon dioxide with triethanolamine in non-aqueous solutions, Korean J. Chem. Eng. 23 (2006) 138–143, https://doi.org/10.1007/BF02705705.
- [40] Cussler, E.L. (2009) Diffusion: mass transfer in fluid systems, Cambridge University Press. ISBN: 9780521871211.
- [41] R. Faiz, M. Al-Marzouqi, Mathematical modeling for the simultaneous absorption of CO₂ and H₂S using MEA in hollow fiber membrane contactors, J. Membr. Sci. 342 (1–2) (2009) 269–278, https://doi.org/10.1016/j.memsci.2009.06.050.
- [42] S. Paul, A.K. Ghoshal, B. Mandal, Removal of CO₂ by single and blended aqueous alkanolamine solvents in hollow-fiber membrane contactor: modeling and simulation, Ind. Eng. Chem. Res. 46 (8) (2007) 2576–2588, https://doi.org/ 10.1021/ie061476f.
- [43] A.T. Nakhjiri, A. Heydarinasab, O. Bakhtiari, T. Mohammadi, The effect of membrane pores wettability on CO₂ removal from CO₂/CH₄ gaseous mixture using NaOH, MEA and TEA liquid absorbents in hollow fiber membrane contactor, Chin. J. Chem. Eng. 26 (9) (2018) 1845–1861, https://doi.org/10.1016/j. ciche.2017.12.012.
- [44] S. Atchariyawut, R. Jiraratananon, R. Wang, Separation of CO₂ from CH₄ by using gas-liquid membrane contacting process, J. Membr. Sci. 304 (1–2) (2007) 163–172, https://doi.org/10.1016/j.memsci.2007.07.030.
- [45] S.P. Yan, M.X. Fang, W.F. Zhang, S.Y. Wang, Z.K. Xu, Z.Y. Luo, K.F. Cen, Experimental study on the separation of CO2 from flue gas using hollow fiber membrane contactors without wetting, Fuel Process. Technol. 88 (5) (2007) 501–511, https://doi.org/10.1016/j.fuproc.2006.12.007.